Available online at www.sciencedirect.com

Chemical Engineering Research and Design

journal homepage: www.elsevier.com/locate/cherd

Potential of superparamagnetic iron oxide nanoparticles coated with carbon dots as a magnetic nanoadsorbent for DNA isolation

Sahand Fakurpur Shirejini, Seyed Mohsen Dehnavi, Mehdi Jahanfar*

Department of Cell and Molecular Biology, Faculty of Life Science and Biotechnology, Shahid Beheshti University, P. O. Box 1983969411, Tehran, Iran

ARTICLE INFO

Article history:
Received 25 August 2022
Received in revised form
16 December 2022
Accepted 5 January 2023
Available online 9 January 2023

Keywords:
DNA extraction
Core-shell
PH-responsive
Superparamagnetic nanoparticles
Solid-phase extraction, Carbon dots

ABSTRACT

In this study, the potential of iron oxide nanoparticles coated with carbon dots (SPION@CDs) as a magnetic nano-adsorbent was studied for DNA bioseparation. The current research reports the core-shell structure of SPION@CDs synthesized using a one-step solvothermal method. The synthesized pH-sensitive SPION@CDs nanohybrid electrostatically isolated DNA at pH= 2 and released it at pH= 8, with a maximum adsorption capacity of 125.12 µg/mg. The method was described by the charge switch of functional groups on the magnetic particle's surface. The Freundlich isotherm model with pseudo-second-order kinetics offered the best fit with R^2 = 0.99. The (3-(4,5-dimethylthiazol-2-yl)– 2,5-diphenyltetrazolium bromide) tetrazolium (MTT) assay results demonstrated that the cell viability of Human foreskin fibroblasts (HFF) stayed above 90% after 24 h at a high concentration (500 µg/mL), showing high biocompatibility and low toxicity of SPION@CDs, which could be a potential candidate for biological applications. The binding ability of the nanohybrids to DNA were determined by electrophoresis and proved that the separation process was successful and the eluted DNA is suitable for subsequent biological processes. The results revealed that the novel nanohybrid (SPION@CDs) is an effective adsorbent for DNA separation due to its low cost, ease of fabrication, high extraction capacity, reusability, and protection of the DNA structure.

1. Introduction

High-quality and efficient DNA extraction is crucial for many molecular biological and genetic studies and DNA-based biomedical applications (Puente-Santiago and Rodríguez-Padrón, 2020; Yıldırım et al., 2022). In addition, DNA adsorption on various surfaces has been widely studied for a variety of applications, including the treatment of autoimmune diseases (Cömert and Odabaşı, 2014), gene therapy (Wolff et al., 1990), DNA vaccination (Tang et al., 1992), cloning (Anderson and Schneider, 2007), and molecular diagnostics of various disorders (Butt and Swaminathan, 2008). As a result, since DNA isolation, protection, and purification are all critical features of DNA-based applications, many researchers have worked to improve the efficiency of DNA isolation techniques (Ali et al., 2022; Kittiborwornkul et al., 2021; Sun et al., 2016). A few techniques for isolating DNA include the cesium bromide-ethidium chloride method, chloroform-phenol extraction, and acetyl trimethyl ammonium bromide (CTAB). However, these methods take a lot of time and effort. Additionally, several techniques make use of potentially carcinogenic chemical reagents or solvents. DNA contamination with RNA, lipids and other molecules obstructing cleavage enzymes and polymerases are common indicators of DNA quality. The extraction process should produce as minimal mechanical stress as possible given the size of the DNA molecule (Maeda et al., 2016; Perçin et al., 2012; Sosa-Acosta et al., 2018). The usage of magnetic solid-

* Corresponding author.
E-mail address: mo_dehnavi@sbu.ac.ir (S.M. Dehnavi).
https://doi.org/10.1016/j.cherd.2023.01.006

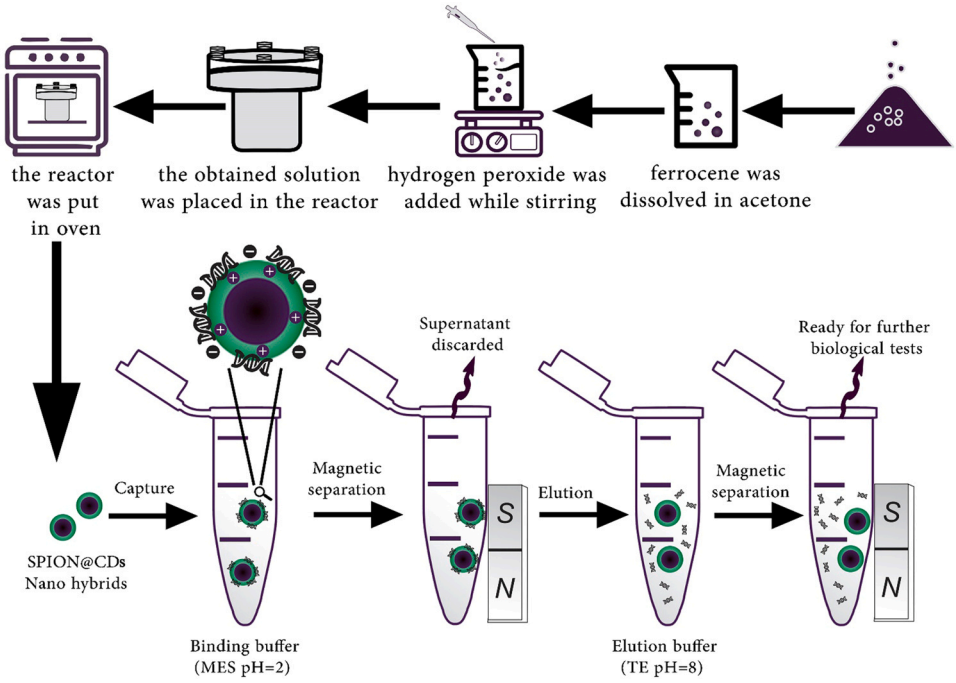

Scheme 1 – Fabrication process of SPION@CDs and isolation procedure of DNA.

phase extraction (MSPE) to extract genomic DNA is growing due to its reduced need for organic solvent, quick processing time, and simplicity of use. This approach avoids the centrifuge cycles that could lead nucleic acids to degrade. Iron oxide magnetic nanoparticles adsorb genomic DNA and enter the solid phase, which can be easily separated by applying a magnetic field. Other advantages of this method over conventional ones include cost, environmental friendliness, and the higher amount and quality of DNA (Fan et al., 2019; Zhang et al., 2019). Nanotechnology is recognized as one of the most remarkable scientific advances of the 21st century, and fast growth of nanostructured biomaterials has been attained from a biomedical point of view (Barjasteh et al., 2022a; Mohsen Dehnavi et al., 2015; Rahnamaee et al., 2022). Carbon dots (CDs), as a new type of carbon-based nanomaterial, have recently gained considerable interest in biological studies, such as drug delivery, bioimaging, wound dressing, and gene transmission, because of their high biocompatibility, low toxicity, pH-responsive functional groups, excellent fluorescence properties, and tunable surface (Rezaei and Ehtesabi, 2022; Tuerhong et al., 2017; Wang and Qiu, 2016). On the other hand, superparamagnetic iron oxide nanoparticles (SPION), Fe_3O_4, have been widely used in magnetic resonance imaging (MRI), targeted drug delivery systems, and magnetic hyperthermia due to their biocompatibility and low toxicity in the human body, reduced oxidation sensitivity, higher magnetic response stability (even up to 50 years), capacity to transfer to superparamagnetic form by reducing particle size, and simplicity of synthesis and surface modification (Ghazanfari et al., 2016; Zasońska and Horák, 2022). A facile one-step solvothermal method was implemented to efficiently fabricate a carbon dots shell and Fe_3O_4 core structure (SPION@CDs) to integrate the properties of carbon dot with Fe_3O_4 NPs (Wang et al., 2014). The fabrication method is based on in situ oxidation and decomposition of the precursor ferrocene with H_2O_2 as a strong oxidizing agent to form the mesoporous carbon shell. This mesoporous carbon dots shell owns a large surface area that can be efficiently protonated in pH= 2 and effectively interacts with the phosphate backbone of DNA. Simultaneously, the magnetic core of the fabricated nanohybrid can readily respond to magnetic field implementation and improve isolation. The magnetic core structure has undergone a different surface modification in prior nano adsorbents, such as polydopamine-modified magnetic nanoparticles (Zhang et al., 2019), chitosan-coated magnetic iron oxide nanoparticles (Pérez et al., 2020), SPION@SiO_2 (Li et al., 2011), and Polyethyleneimine (PEI)@$FePO_4$ (Hu et al., 2015), which requires time, cost, and also reduces the efficiency of the DNA isolation. In this study, we developed a core-shell structure using a one-step solvothermal approach that could isolate DNA electrostatically at high rates and whose surface functional groups could be activated by pH lowering. Additionally, SPION@CDs nanohybrids may easily release DNA by raising the pH of the solution, and the DNA could then be used for additional biological testing.

2. Materials and methods

2.1. *Materials*

The chemical reagents, such as Ferrocene ($Fe(C_5H_5)_2$, > 98%), hydrogen peroxide (H_2O_2, 30%), acetone (C_3H_6O), ethylenediaminetetraacetic acid disodium salt (EDTA, > 99%), Tris (hydroxymethyl) aminomethane (Trometamol), sodium chloride (NaCl, 99.8%), sodium hydroxide (NaOH, 99%), ethanol 70%, Hydrochloric acid (HCl, 25%), and 4-Morpholineethanesulfonic acid (MES, 95%) were purchased from Merck and used as supplied without any further purification. DNA from the calf thymus (CT DNA) was obtained from Sigma-Aldrich. The water used in all experiments was Millipore Milli-Q grade. Roje kit (Tehran-Iran) was used to achieve cellular extract.

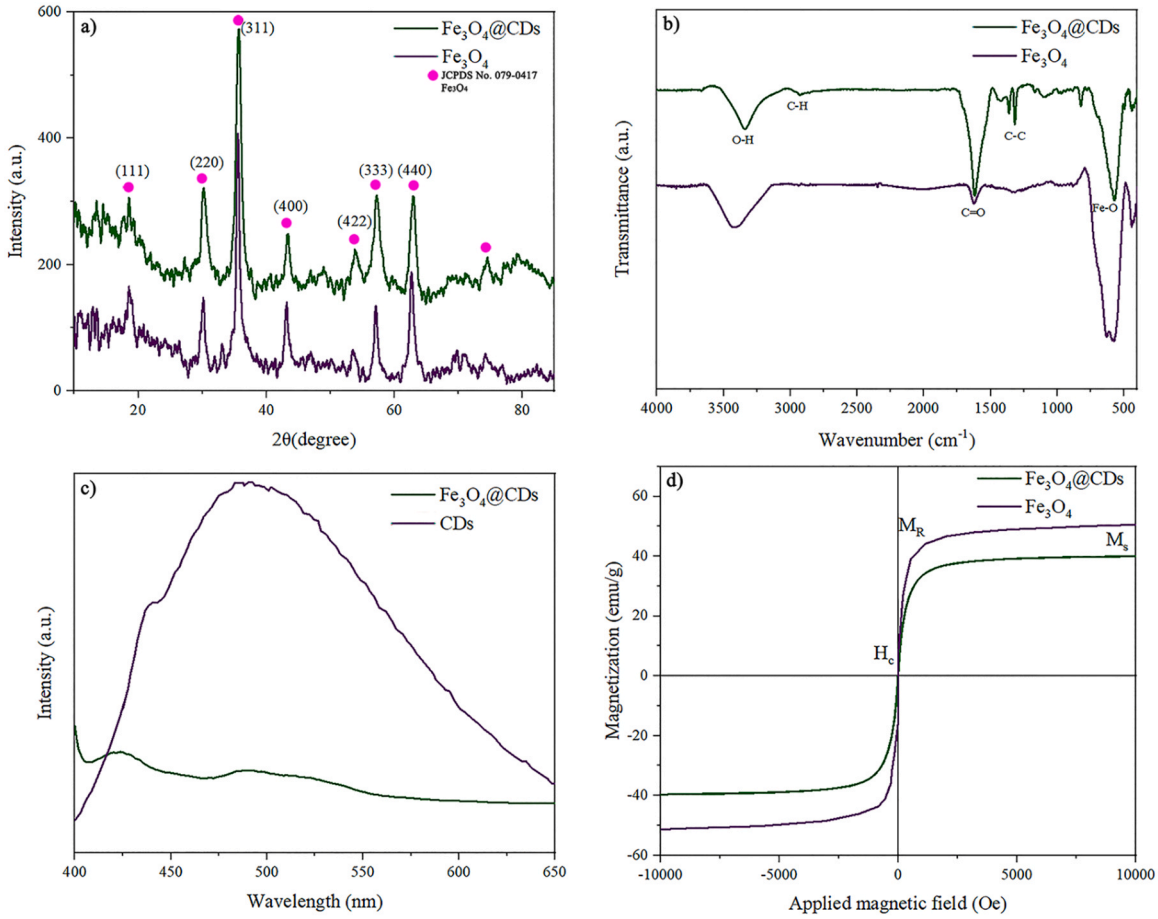

Fig. 1 – a) The XRD pattern of as fabricated SPION and SPION@CDs, b) FTIR spectra of SPION and SPION@CDs, c) PL emission spectra of CDs and SPION@CDs, d) magnetic properties of SPION and SPION@CDs under a magnetic field ranged from −10 to + 10 kOe at 300 K.

2.2. *Preparation of SPION@CDs nanohybrid*

The SPION@CDs nanocomposite was prepared using a one-step solvothermal method (Wang et al., 2014). 100 mg ferrocene was dissolved in 30 mL acetone and sonicated for 30 min. Next, 5 mL of 30% H_2O_2 solution was slowly added to the stated solution and rapidly stirred for 30 min. The solution was transferred to a Teflon-lined stainless-steel autoclave at 200 °C for 48 h (Scheme 1). A dark brown solution was attained. As the autoclave naturally cooled to ambient temperature, the products were washed with acetone and separated magnetically by a neodymium magnet. The supernatant was discarded after the third round of washing, and the dark brown precipitate was allowed to air dry at room temperature.

2.3. *Characterization of SPION@CDs*

The composition and the crystal structure of SPION@CDs were investigated by XPert Pro MPD with a voltage of 40 kV and 40 mA current. The surface chemistry of nanohybrid was evaluated through FTIR (Bruker Tensor27) in the range of 400–4000 cm^{-1}. The Fluorescence Spectrometer (PerkinElmer) in the range 200–900 nm was used to demonstrate the photoluminescence properties of the carbon dots attached to the magnetic core. Magnetic characteristics of SPION@CDs were evaluated on a vibrating sample magnetometer LBKFB of Kashan Kavir in a magnetic field ranging from −10 to + 10 kOe at 300 K. The morphology and size of SPION@CDs were studied with JSM-7610 F scanning electron microscopy and EM 208 S transmission electron microscope. The surface electrical charge was measured using the Zetasizer Nano ZS (red badge) ZEN 3600 device. The DNA adsorption studies were calculated by a NanoDrop (Nabi UV/Vis Nano Spectrophotometer) at 260 nm.

2.4. *DNA adsorption studies on SPION@CDs*

The calf thymus DNA model was used to test DNA adsorption capacities of fabricated SPION@CDs. The stock DNA was dissolved in sterile deionized water to create a standard DNA solution (800 ng/μL). Then, a 1.5 mL microtube containing 16 μL of DNA, 84 μL of binding buffer (MES), and 24 μg of SPION@CDs solution was mixed to make a total volume of 100 μL. The mixture was gently taped at room temperature for 10 min. Subsequently, an external magnet was employed for magnetic separation. Afterward, 3 μL of the supernatant was carefully collected for UV analysis on a Nanodrop at 260 nm. The amount of adsorbed DNA was estimated by subtracting the amount from a reference before magnetic adsorption. Scheme 1 demonstrates the extraction procedure of DNA. The extraction capacity (Qe (μg/mg)) was calculated using the following equation (Barjasteh et al., 2023).

$$Q_e = \frac{(C_0 - C) \times V}{m} \quad (1)$$

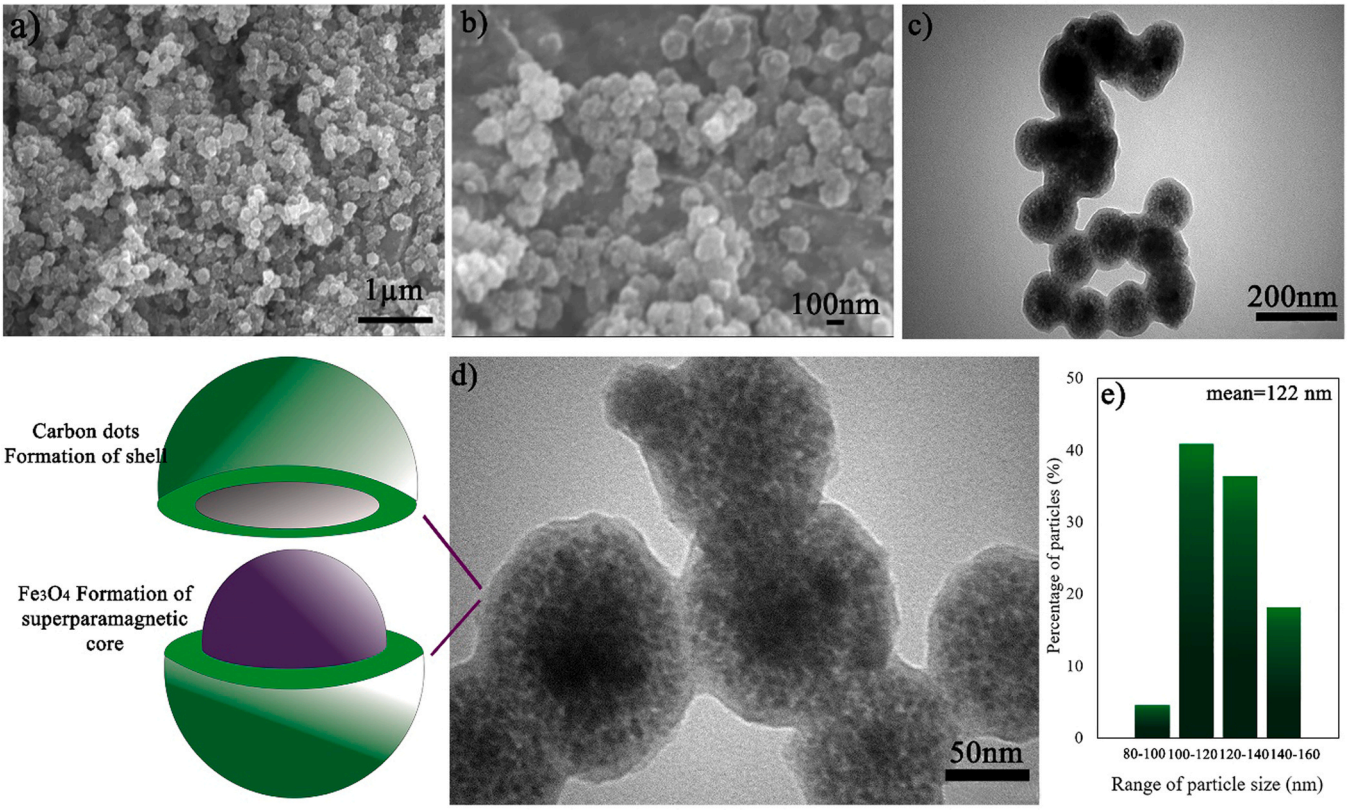

Fig. 2 – (a and b) FESEM, (c and d) TEM images, and e) size distribution diagram of SPION@CDs core-shell structure.

C_0 (μgμL^{-1}) and C (μgμL^{-1}) are the initial and equilibrium concentrations of DNA in the solution, respectively. V (μL) is the total volume of the prepared solution and m (mg) is the quantity of SPION@CDs.

2.5. *Regeneration studies*

After DNA isolation, the fabricated SPION@CDs was retrieved by magnetic field, dissolved in 30 μL of TE buffer solution (10 mM Tris-HCl and 1.0 mM EDTA at pH=8), and gently tapped at room temperature for 10 min in the recycling process. Before being dried for further use, the regenerated SPION@CDs nanohybrid was washed three times with water and ethanol 70%. The isolation-elution cycles were repeated five times to demonstrate the regeneration potential of SPION@CDs.

2.6. *Extracted DNA characterization*

The integrity of recovered CT DNA after desorption was determined using agarose gel electrophoresis. The agarose gel was made at a 1% concentration. After the desorption process, 10.0 μL of the solution was injected into the gel, and a 15-minute electrophoresis operation was performed at 100 V. DNA was marked with Safe stain and Loading buffer 6x before being revealed with UV light. Also, Human whole blood was used to evaluate the extraction efficiency of SPION@CD in actual samples. To gain cellular extract Roje kit (Tehran-Iran) was used. 800 ng of SPION@CD was added to a 1.5 mL Eppendorf tube containing 300 μL the binding buffer (10 mM MES-HCl, pH=2) and 150 μL of cell lysate. The mixture was gently taped at room temperature for 10 min. Subsequently, an external magnet was employed for magnetic separation and the same procedure as used for CT DNA was performed.

2.7. *Cell cytotoxicity assessment*

The in vitro cytotoxicity of SPION@CDs was evaluated using an MTT colorimetric test in 96-well plates. Each well was cultivated with a sufficient number of HFF-1 cells (5000), allowing the cells to cling to the plate's bottom and become stable. The cells were then treated for 24 h with SPION@CDs concentrations of 15.6, 31.2, 62.5, 125, 250, and 500 g/mL. SPION@CDs-free cells were present in the control samples. After the incubation period, the supernatant was removed, and each well received 100 μL of MTT solution diluted PBS (5 mg/mL), which was added in the dark and incubated for 4 h at 37 °C in 5% CO_2. After dissolving the formazan crystals in DMSO, the optical absorbance of the resulting solution was determined at 570 nm using a plate reader (EPOCH-Biotek, USA) to determine the proportion of viable cells. The equation below was used to calculate the percentage of cell viability, where OD_{sample} and $OD_{control}$ stand for the optical densities of the sample and control, respectively.

$$\text{Cell viability}(\%) = \frac{OD_{sample}}{OD_{control}} \times 100 \quad (2)$$

3. Results and discussion

3.1. *Characterization of SPION@CDs nano hybrids*

The XRD patterns of SPION and SPION@CDs nanohybrids (Fig. 1a) exhibit diffraction peaks at 2θ = 18.3, 30.1, 35.4, 43.1, 53.4, 56.9, and 62.8, which can be entrusted to (111), (220),

Table 1 – Zeta potential of SPION and SPION@CDs at different pH values.

Nano particles	SPION (pH = 7)	SPION@CDs (pH = 7)	SPION@CDs (pH = 2)
Zeta potential(mV) ± SD	-8.55 ± 2.35	-28.7 ± 1.38	18.4 ± 1.71

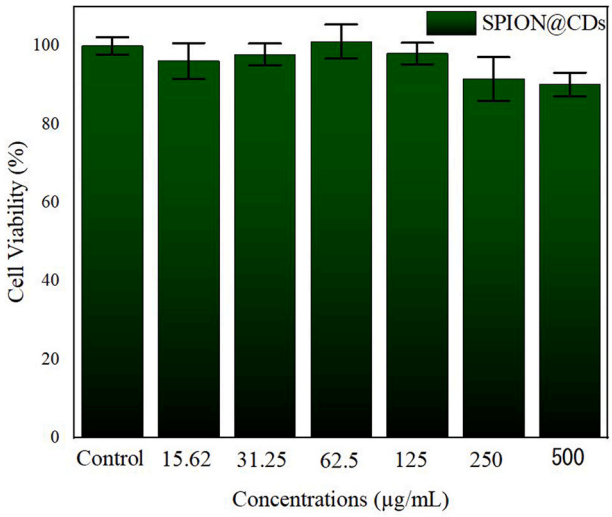

Fig. 3 – Cell viability of the HFF-1 cell line in different concentrations of SPION@CDs (15.6, 31.2, 62.5, 125, 250, and 500 µg/mL) after 24 h incubation.

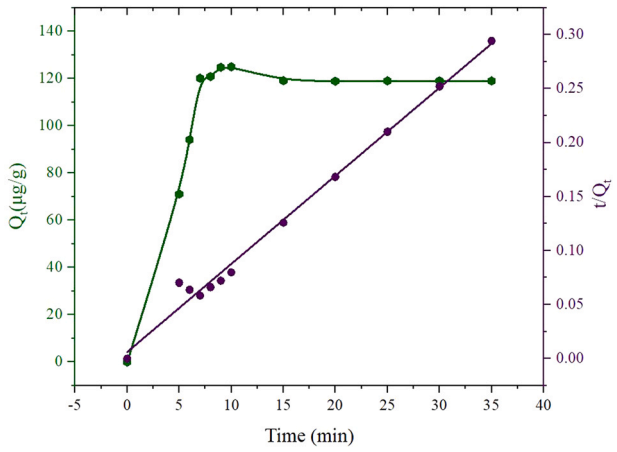

Fig. 4 – Effect of contact time on the DNA extraction (green) and the pseudo-second-order model for the DNA isolation kinetics (purple) by SPION@CDs.

(311), (400), (422), (333), and (440) SPION planes, respectively, suggesting that iron oxide NPs were pure with a cubic spinel structure in SPION@CDs nanohybrids. These peaks are well-matched with the standard JCPDS card no. 079–0417 Fe_3O_4. The low concentrations, low crystallinity, and high dispersion of CDs in the SPION@CDs nanohybrids account for the lack of any CDs-related signal (Alvand and Shemirani, 2017a).

Fig. 1b depicts the FTIR spectra of SPION and SPION@CDs to study the functional groups. The Fe—O vibrational bond is found at 556 cm^{-1} (Duffy et al., 2012). The characteristic peaks at 3334 cm^{-1} and 1615 cm^{-1} correspond to the stretching mode of —OH and C═O groups, respectively, belonging to water absorption (Ghanbari et al., 2021a) and carboxylic acid groups conjugated with condensed aromatic carbons. The C—C and C—H stretching bands are positioned at 1400 cm^{-1} and 2928 cm^{-1}, respectively (Ghanbari et al., 2021b). The distinct peaks belong to carbon-containing functional groups, demonstrating the attachment of carbon dots on the SPION core surface. Furthermore, as observed in Fig. 5b, the FTIR spectrum of SPION shows the absorption peaks at 556 cm^{-1}, 1615 cm^{-1}, and 3334 cm^{-1}, which belong to the Fe—O, C═O, and –OH groups, respectively (Alvand and Shemirani, 2017b; Zhang et al., 2021).

The emission spectra of CDs and SPION@CDs are depicted in Fig. 1c. The PL spectra revealed that the fluorescence intensity of CDs is quenched by adding SPION. The surface quenching of fluorescence is due to the coating of CDs over iron oxide. CDs have a considerable fluorescence selectivity for Fe^{3+} ions because of the rapid electron transfer between Fe^{3+} and CDs surface-passivated with oxygen-rich groups. Besides, the fluorescence of CDs fades because of the non-radiative electron/hole recombination (Alaghmandfard and Madaah Hosseini, 2021). Two principal explanations are suggested in the PL of CDs. It is possible to extract the surface/edge state in CDs that describes how armchair and zigzag edges form when graphene is cutting in various directions. A more critical factor in the electrical attributes of CDs is edge type. Therefore, the fabrication process and raw materials are crucial to the electrical characteristics of CDs. Quantum confinement in CDs is credited with causing the second. Numerous factors, including passivation, size (quantum effect), surface groups, defects, and the recombination of electron-hole pairs localized inside sp^2 carbon buried in an sp^3 matrix, have been suggested as the causes of the PL of CDs (Gao et al., 2016; Liu et al., 2015).

The magnetic properties of SPION and SPION@CDs were studied at room temperature in an applied magnetic field, as revealed in Fig. 1d. The saturation magnetization of SPION and SPION@CDs was 50.4 emu/g and 39.9 emu/g, respectively, which is insignificantly lower than reported values of 51.2 emu/g and 44.5 emu/g for SPION nanoparticles and SPION@SiO_2, respectively (Du et al., 2006). The difference could be due to the shell thickness that surrounded these nanoparticles. Nanohybrids demonstrated agile magnetic response and superior water solubility after removing the magnetic field. No remanence or coercivity was observed at room temperature, showing the superparamagnetic behavior of SPION@CDs (Bean et al., 1959; Feng et al., 2011), which is required for bioseparation (Amiri et al., 2021; Moradi et al., 2022).

The morphology of the SPION@CDs was studied using SEM and TEM as presented in Fig. 2. Fig. 2 reveals the sphere-like nanoparticles with high dispersity, which are almost uniform in size and shape. The TEM images prove the structure and morphology of the core-shell. The nanohybrids are composed of SPION nanocrystals packed in the core region and carbon dots surrounding them. Fig. 2e depicts the size distribution diagram of SPION@CDs with an average diameter of 122 nm estimated by Digimizer software from TEM images.

Table 1 shows the surface electric charge of as-prepared samples. The negative electric charge of the NPs in distilled water was reported as −28.7 ± 1.38 mV based on the

Table 2 – Kinetic model constants for DNA adsorption onto SPION@CDs.

Models	Pseudo-second-order model			Pseudo-first-order model		
	K_1 (min^{-1})	R^2	Q_e (μg/mg)	K_2 (g/μg·min)	R^2	Q_e (μg/mg)
DNA adsorption onto SPION@CDs	−0.0107	0.34	10.28	0.0108	0.99	121.95

functional carboxylate groups on the surface of SPION. SPION@CDs can electrostatically bind to positively charged drugs and biomolecules in a neutral pH solution. The difference in zeta potential values in neutral pH between SPION (–8.55 ± 2.35 mV) and SPION@CDs (–28.7 ± 1.38 mV) confirms the attachment of carbon dots on the surface of SPION due to carboxylic group abundance (Feng et al., 2011; Zhu et al., 2008). SPION@CDs gain a positive electric charge (18.4 ± 1.71 mV) in an acidic medium (pH=2) due to the protonation of their functional groups and are ready to bind electrostatically to the phosphate backbone of DNA. These results show that hydrophilic functional groups are abundant on the nanoparticle surface, which not only can lead to high solubility in an aqueous medium but also plays a crucial role in interaction with biomolecules, drugs, and other coatings.

Cell toxicity play a significant role in applying magnetic nanoparticles in bioseparation, contrast agents, and drug delivery (Aggarwal et al., 2009; Naahidi et al., 2013). Fig. 3 displays the viability of the cells after being incubated with different concentrations of SPION@CDs (15.6, 31.2, 62.5, 125, 250, and 500 μg/mL). The viability of HFF-1 cells remained above 90% after 24 h of incubation at a concentration of 500 μg/mL. The MTT outcomes demonstrated that SPION@CDs show high biocompatibility, low toxicity, and promise for use in biological applications.

3.2. *DNA adsorption studies*

The effects of exposure time on the DNA adsorption capacity of SPION@CDs were initially studied over time while maintaining a total volume of 30 μL, which included 4.2 ng/μL CT DNA, 800 ng SPION@CDs, and a 10 mM MES-HCl (pH=2) binding solution. The adsorption rate of SPION@CDs increased sharply within 10 min due to the presence of many vacant active sites and then fluctuated very little, with no additional adsorption occurring after 35 min. Therefore, the incubation time was selected to be 10 min for further experiments. As seen in Fig. 4, the adsorption of DNA on SPION@CDs has an equilibrium time of 35 min. Pseudo-first-order (Eq. (3)) and pseudo-second-order (Eq. (4)) kinetic models define the adsorption kinetics model and are mathematically listed as follows:

$$\ln(Q_e - Q_t) = \ln Q_e - K_1 t \tag{3}$$

$$\frac{t}{Q_t} = \frac{1}{K_2 Q_e^2} + \frac{t}{Q_e} \tag{4}$$

Where Q_e and Q_t (μg/mg) are the DNA binding quantities at equilibrium and at t time (min), respectively; K_1 (min^{-1}) and K_2 (g/μg·min) are the pseudo-first-order and pseudo-second-order rate constants, respectively. Fig. 4 illustrates the results of the pseudo-second-order kinetic model, and Table 2 lists the kinetic parameters. As shown by the pseudo-second-order model's R^2 values (0.99), which are closer to 1 than those of the pseudo-first-order model, the pseudo-second-order kinetic model is better suited to describe the SPION@CDs extraction kinetics.

The pseudo-second-order model's Qe (121.9 μg/mg) and the real Qe (119 μg/mg) are practically equal. According to this model, the isolation process is regulated by chemical adsorption, which also involves the electrostatic attraction between magnetic nanohybrids and DNA. The pH of the binding buffer plays a crucial role in the DNA isolation process. SPION@CDs are positively charged in the binding solution, as shown in Table 1 (10 mM MES-HCl, pH=2). As shown in Table 1, the binding solution causes the SPION@CDS to become positively charged (10 mM MES-HCl, pH=2). DNA was negatively charged at pH > 1 due to the deprotonation of phosphate groups [35]. Therefore, electrostatic interaction caused the positively charged SPION@CD to attract the negatively charged DNA. Additionally, as indicated in Fig. 1, other types of interactions such as hydrogen bonds and Van der Waals forces, could be anticipated due to the other active functional groups on the surface of SPION@CDs, including

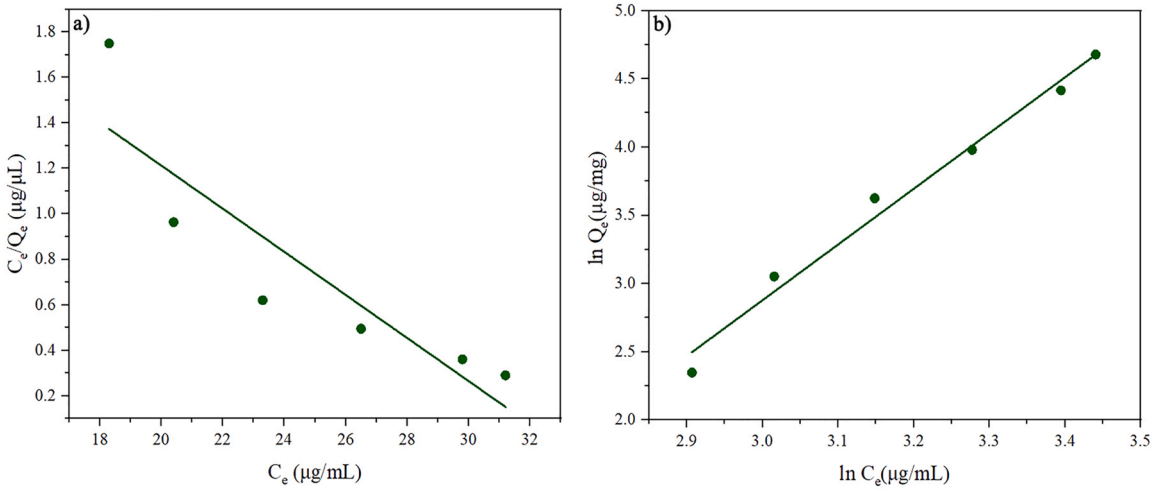

Fig. 5 – a) Langmuir and b) Freundlich isotherms for the DNA isolation onto SPION@CDs.

Table 3 – Comparison of the maximum adsorption capacities of several different adsorbents.

Adsorbents	Binding buffer	Elution buffer	Extraction time	Adsorbance capacity (μg/mg)	Ref.
SPION@CDs	10 mM 4.0-Morpholineethanesulfonic acid (MES) at pH= 2.0	10 mM Tris-HCl and 1.0 mM EDTA at pH= 8.0	10 min	125.1	This work
Polydopamine@SPION	20% (w/v) PEG and NaCl 4.0 M at pH2.0	10 mM Tris–HCl and 1.0 mM EDTA at pH= 8.0	10 min	116.7	(Zhang et al., 2019)
Polyethyleneimine@$FePO_4$	0.3 mol L-1 MgCl2 and 0.01 mol L-1 Britton–Robinson BR buffer at pH= 4.0	Britton–Robinson (BR) buffer solution at pH= 10	30 s	61.9	(Hu et al., 2015)
Chitosan@SPION	Phosphate buffer pH = 4.8	Phosphate buffer at pH = 9.0	120 min	98.0	(Pérez et al., 2020)
Zirconia@SPION	(HCl/KCl) at pH= 2.0	Britton–Robinson (BR) buffer solution	5 min	53.5	(Saraji et al., 2017)
Polydopamine (PDA)@poly(2-hydroxypropylene imines)@SPION	DNA solution (50 μg/mL), at pH = 4.0	DNA solution (50 μg/mL), at pH = 6.0	10 min	153.3	(Pan et al., 2019)

carboxyl and hydroxyl. The cellular extract is a mixture of several components, such as proteins, carbohydrates, lipids, and nucleic acids. Most proteins have an isoelectric point of more than 4.0. They carry a positive charge in the solution with pH values lower than their isoelectric point (Barjasteh et al., 2022b). Therefore, the adsorption of proteins on the sorbent is very low in an acidic solution due to the positive charge of the surface (Hu et al., 2015). Also, important cellular carbohydrates such as D-glucose, D-galactose, D-mannose, D-fructose, etc., have an isoelectric point of more than 10 (Rendleman, 1973). Lipids break down in an acidic environment, like the medium used in this study, and the constituents gain a positive charge to repulse the SPION@CD (Kolter and Sandhoff, 2010; Lieckfeldt et al., 1995). That's why most of the research used acidic binding buffers to separate DNA specifically. Based on these considerations, pH 2 was selected for DNA adsorption in this study.

The impact of DNA concentration was evaluated on adsorption capacity. Fig. 5 shows the SPION@CDs extraction results at various DNA concentrations. The findings indicate that the adsorption capacity of SPION@CDs was directly correlated with DNA concentration. As the DNA concentration raised, the adsorption capacity rose. It is owing to a higher pressure induced by a higher DNA concentration, which facilitates mass transfer between liquid and solid phases of nanohybrids. Table 3 lists the maximum adsorption capacities of several various adsorbents. As can be seen, SPION@CDs can compete with other adsorbents due to their maximum adsorption capacity of 125.12 μg/mg. The surface structure of magnetic nanohybrids and isolation behavior of the extraction systems were all characterized using equilibrium adsorption isotherms. The Langmuir (Eq. (5)) and Freundlich (Eq. (6)) models were applied for this purpose, which are given in linear form as follows:

$$\frac{C_e}{Q_e} = \frac{1}{K_L Q_m} + \frac{C_e}{Q_m} \quad (5)$$

$$\ln Q_e = \frac{1}{n}\ln C_e + \ln K_F \quad (6)$$

C_e (μg/mL) and Q_e (μg/mg) are the DNA equilibrium concentration and the associated quantity of DNA on the nanohybrids, respectively. Q_m (μg/mL) is the theoretical saturated maximum loading capacity, while K_L(mL/μg) is the Langmuir constant engaged in the affinity of active binding sites. The Freundlich constant (K_F) and n are correlated to the binding capacity and extraction efficiency of SPION@CDs, respectively.

Langmuir and Freundlich isotherm models were conducted to describe isothermal data at different concentrations, as shown in Figs. 5a and 5b, respectively, and the relative parameters are reported in Table 4. Freundlich isotherm may accurately represent the DNA isolation mechanism onto SPION@CDs since R^2 obtained from the Freundlich isotherm model (0.9839) is higher than Langmuir model (R^2 =0.7993) at different concentrations. The results express multilayer adsorption, having a heterogeneous surface and a non-uniform distribution of adsorption heat and affinities (Adamson and Gast, 1967). According to the surface chemistry of the nanohybrids, which is composed of few chemical functional groups, we could suggest a heterogeneous surface. In this study, the value of n was 0.244. According to Freundlich's theory, the adsorption isotherm becomes valuable when $n < 1$ (Tran et al., 2017).

Table 4 – Langmuir and Freundlich adsorption isotherm model parameters for the DNA adsorption onto SPION@CDs.

Isotherm models	Langmuir			Freundlich		
	K_L (min^{-1})	R^2	Q_m (min^{-1})	K_F (μg/mg·min)	R^2	$\frac{1}{n}$
DNA	0.90	0.79	0.32	8.44×10^{-5}	0.98	4.08

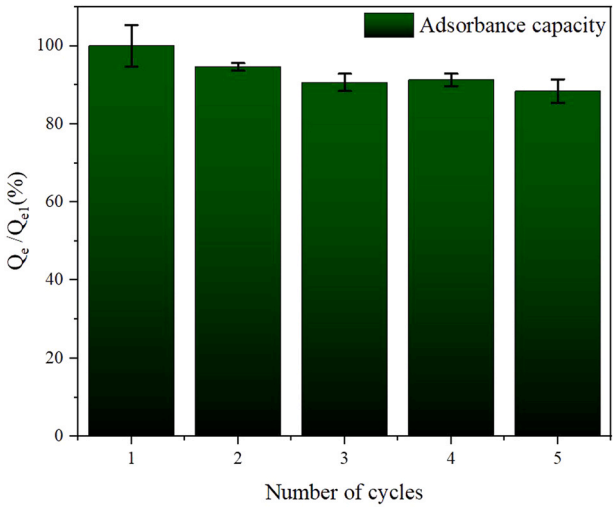

Fig. 6 – Recycled test for the DNA extraction on SPION@CDs.

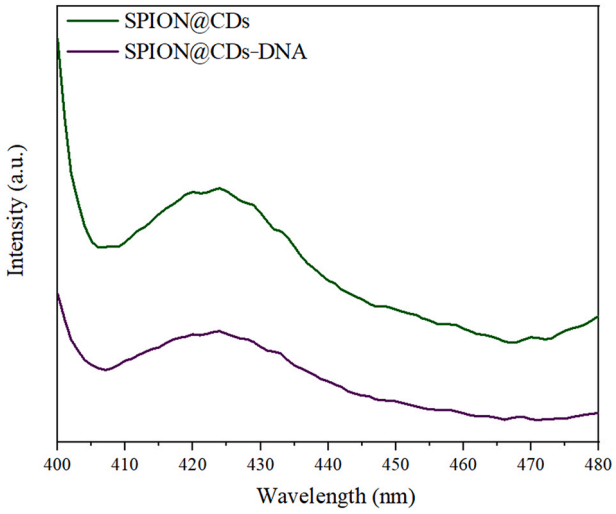

Fig. 7 – PL emission spectrum of SPION@CDs in the range of 400–480 nm.

Furthermore, a calculation of 1/n yielded a value of 4.08, which is higher than the unit and suggests cooperative adsorption (Haghseresht and Lu, 1998).

3.3. *Regeneration test*

The commercialization and practical application of adsorbents depend heavily on their ease of regeneration and reusability. The reusability of SPION@CDs was assessed for DNA adsorption over five consecutive cycles by washing SPION@CDs with a TE buffer. Fig. 6 shows the variations in DNA adsorption capacity onto magnetic nanoparticles after five adsorption-desorption cycles. The results exhibit no considerable drop in adsorbance capacity, and the adsorption capacity is 90% of the initial adsorption capacity after five adsorption-desorption cycles. It is inferred that SPION@CDs have a stable composition that maintains its structure through the binding and elution process, resulting in the reusability of the SPON@CDs.

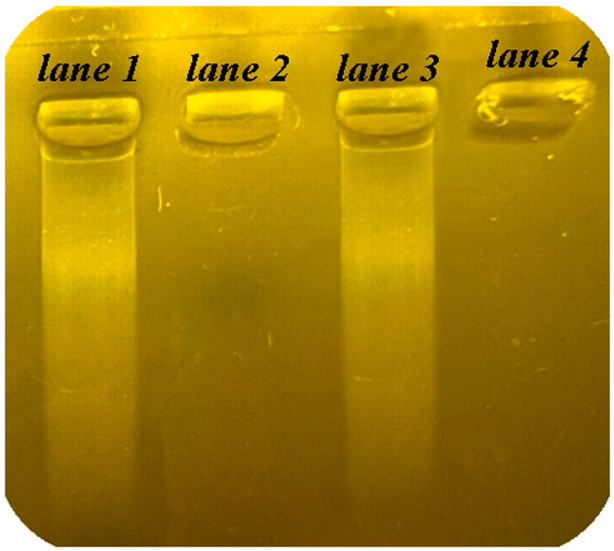

Fig. 8 – Agarose gel electrophoresis of calf thymus DNA isolated using SPION@CDs. Lane 1 = DNA control solution; Lane 2 = binding buffer; Lane 3 = elution buffer with desorbed DNA, and Lane 4 = SPION@CDs in binding buffer.

A photoluminescence spectrometer was implemented to specifically prove the presence of carbon dots on the surface of the mesoporous SPION. Despite SPION, CDs often exhibit PL quantum yields and present a distinct shift in their emission spectrum with excitation wavelength. As shown in Fig. 7, SPION@CDs showed an emission of around 425 nm (Resch-Genger et al., 2008). This could be great explanation for the presence of carbon dots on the surface of SPION. In addition, PL emission of CDs was noticeably quenched by the interaction between SPION@CDs and DNA at the same concentration (240 ng/mL), proving the attachment of DNA to SPION@CDs.

3.4. *Analyzing retrieved DNA by electrophoresis*

Verifying that the desorption process occurred and did not jeopardize the structural integrity of DNA is crucial. In this regard, the desorbed DNA was subjected to agarose gel electrophoresis (Fig. 8). The intact DNA control sample was placed in lane 1. Line 2 is related to the supernatant of the binding process (binding buffer). As can be seen, there is no sign of residual DNA in the binding buffer, and the nanohybrids have effectively adsorbed DNA. The supernatant was inserted in lane 3 after elution with TE buffer at pH= 8, demonstrating that the SPION@CDs desorbed DNA at higher pH

and the desorbed DNA is similar to the control one. SPION@CDs eluted in binding buffer (10 mM MES-HCl, pH=2) were loaded in lane 4, demonstrating no sign of DNA. Likewise, there is evidence of DNA degradation in the bands associated with the eluted DNA smear, which can be due to the presence of degraded DNA. However, the DNA control band likewise exhibits the DNA smear. Since the band patterns in lanes 1 and 3 are nearly identical and present in the control sample, the degradation is not because of the isolation process. Similarly, genomic DNA from human whole blood was used to assess the extraction efficiency of SPION@CD in actual samples. As shown in Fig. S1, the genomic DNA control sample was loaded in lane 1. The supernatant of the binding process is addressed in Line 2. As can be seen again, there is no trace of remaining DNA in the binding buffer, proving the nanohybrid's potential for adsorption. After elution with TE buffer at pH 8, the supernatant was loaded in lane 3, demonstrating that the SPION@CDs and pH value of 2 didn't affect the DNA's integrity and that the desorbed DNA was similar to the control DNA. SPION@CDs loaded in lane 4 showed no evidence of DNA after being eluted in binding buffer (10 mM MES-HCl, pH=2). Based on the findings, it can be concluded that the isolation process was accomplished well and shows that the eluted DNA is suitable for subsequent biological operations.

4. Conclusions

In conclusion, core-shell superparamagnetic iron oxide nanoparticles coated with carbon dots (SPION@CDs) were fabricated utilizing a one-step solvothermal approach. The TEM images prove the structure and morphology of the core-shell. According to the VSM results, SPION@CDs show superparamagnetic behavior, which is desirable for biological applications. The pseudo-second-order kinetics and Freundlich isotherm model confirmed that SPION@CDs could electrostatically capture DNA, which was also supported by the positive zeta potential at pH= 2. The highest DNA adsorption capacity of 125.12 µg/mg was achieved using MES (10 mM, pH=2) as the binding buffer for 10 min as the ideal adsorption period. This value was higher than other materials under the same extraction circumstances. The experimental data fit well with the Freundlich isotherm and pseudo-second-order kinetics models. After five usage cycles, SPIOIN@CDs continued to exhibit excellent biocompatibility and maintain a high isolation capacity. Agarose gel electrophoresis demonstrates that the adsorption/desorption procedure does not alter the DNA structure. Moreover, the interaction of SPION@CDs with DNA significantly reduced the photoluminescence emission of C-dots, indicating that it has a great deal of promise in biosensor applications. The unique properties of SPION@CDs nanohybrid make it an attractive candidate for DNA bioseparation, applications.

Declaration of Competing Interest

The authors declare that they have no known competing financial interests or personal relationships that could have appeared to influence the work reported in this paper.

Appendix A. Supporting information

Supplementary data associated with this article can be found in the online version at doi:10.1016/j.cherd.2023.01.006.

References

Adamson, A.W., Gast, A.P., 1967. Physical chemistry of surfaces. Interscience publishers, New York.
Aggarwal, P., Hall, J.B., McLeland, C.B., Dobrovolskaia, M.A., McNeil, S.E., 2009. Nanoparticle interaction with plasma proteins as it relates to particle biodistribution, biocompatibility and therapeutic efficacy. Adv. Drug Deliv. Rev. 61, 428–437.
Alaghmandfard, A., Madaah Hosseini, H.R., 2021. A facile, two-step synthesis and characterization of Fe3O4–LCysteine–graphene quantum dots as a multifunctional nanocomposite. Appl. Nanosci. 11, 849–860.
Ali, T.H., Mandal, A.M., Heidelberg, T., Hussen, R.S.D., 2022. Sugar based cationic magnetic core–shell silica nanoparticles for nucleic acid extraction. RSC Adv. 12, 13566–13579.
Alvand, M., Shemirani, F., 2017a. A Fe3O4@ SiO2@ graphene quantum dot core-shell structured nanomaterial as a fluorescent probe and for magnetic removal of mercury (II) ion. Microchim. Acta 184, 1621–1629.
Alvand, M., Shemirani, F., 2017b. A Fe3O4@SiO2@graphene quantum dot core-shell structured nanomaterial as a fluorescent probe and for magnetic removal of mercury(II) ion. Microchim. Acta 184, 1621–1629.
Amiri, M., Khazaeli, P., Salehabadi, A., Salavati-Niasari, M., 2021. Hydrogel beads-based nanocomposites in novel drug delivery platforms: recent trends and developments. Adv. Colloid Interface Sci. 288, 102316.
Anderson, R.J., Schneider, J., 2007. Plasmid DNA and viral vector-based vaccines for the treatment of cancer. Vaccine 25, B24–B34.
Barjasteh, M., Dehnavi, S.M., Ahmadi Seyedkhani, S., Rahnamaee, S.Y., Golizadeh, M., 2022a. Synergistic wound healing by novel Ag@ ZIF-8 nanostructures. Int. J. Pharm. 629, 122339.
Barjasteh, M., Vossoughi, M., Bagherzadeh, M., Pooshang Bagheri, K., 2022b. Green synthesis of PEG-coated MIL-100(Fe) for controlled release of dacarbazine and its anticancer potential against human melanoma cells. Int. J. Pharm. 618, 121647.
Barjasteh, M., Vossoughi, M., Bagherzadeh, M., Pooshang Bagheri, K., 2023. MIL-100(Fe) a potent adsorbent of dacarbazine: experimental and molecular docking simulation. Chem. Eng. J. 452, 138987.
Bean, C., DeBlois, R., Nesbitt, L., 1959. Eddy-current method for measuring the resistivity of metals. J. Appl. Phys. 30, 1976–1980.
Butt, A.N., Swaminathan, R., 2008. Overview of circulating nucleic acids in plasma/serum: update on potential prognostic and diagnostic value in diseases excluding fetal medicine and oncology. Ann. N. Y. Acad. Sci. 1137, 236–242.
Cömert, Ş.C., Odabaşı, M., 2014. Investigation of lysozyme adsorption performance of Cu2+-attached PHEMA beads embedded cryogel membranes. Mater. Sci. Eng.: C. 34 (1–8).
Du, G.-H., Liu, Z., Xia, X., Chu, Q., Zhang, S., 2006. Characterization and application of Fe3O4/SiO2 nanocomposites. J. Sol. -Gel Sci. Technol. 39, 285–291.
Duffy, P., Magno, L.M., Yadav, R.B., Roberts, S.K., Ward, A.D., Botchway, S.W., Colavita, P.E., Quinn, S.J., 2012. Incandescent porous carbon microspheres to light up cells: solution phenomena and cellular uptake. J. Mater. Chem. 22, 432–439.
Fan, Q., Guan, Y., Zhang, Z., Xu, G., Yang, Y., Guo, C., 2019. A new method of synthesis well-dispersion and dense Fe3O4@ SiO2 magnetic nanoparticles for DNA extraction. Chem. Phys. Lett. 715, 7–13.
Feng, J., Mao, J., Wen, X., Tu, M., 2011. Ultrasonic-assisted in situ synthesis and characterization of superparamagnetic Fe3O4 nanoparticles. J. Alloy. Compd. 509, 9093–9097.
Gao, X., Du, C., Zhuang, Z., Chen, W., 2016. Carbon quantum dot-based nanoprobes for metal ion detection. J. Mater. Chem. C. 4, 6927–6945.
Ghanbari, M., Salavati-Niasari, M., Mohandes, F., 2021a. Injectable hydrogels based on oxidized alginate-gelatin reinforced by carbon

nitride quantum dots for tissue engineering. Int. J. Pharm. 602, 120660.
Ghanbari, M., Salavati-Niasari, M., Mohandes, F., 2021b. Thermosensitive alginate–gelatin–nitrogen-doped carbon dots scaffolds as potential injectable hydrogels for cartilage tissue engineering applications. RSC Adv. 11, 18423–18431.
Ghazanfari, M., Kashefi, M., Shams, S., Jaafari, M., 2016. Perspective of Fe3O4 nanoparticles role in biomedical applications. Biochem Res Int 2016, 7840161.
Haghseresht, F., Lu, G., 1998. Adsorption characteristics of phenolic compounds onto coal-reject-derived adsorbents. Energy Fuels 12, 1100–1107.
Hu, L.-L., Hu, B., Shen, L.-M., Zhang, D.-D., Chen, X.-W., Wang, J.-H., 2015. Polyethyleneimine–iron phosphate nanocomposite as a promising adsorbent for the isolation of DNA. Talanta 132, 857–863.
Kittiborwornkul, N., Sahithi, S.A., Phetsom, J., Phusantisampan, T., Pongprayoon, W., Sriariyanun, M., 2021. Comparative evaluation of DNA extraction from rice's root-associated bacterial consortium for population structure study, E3S Web of Conferences. EDP Sci. 02014.
Kolter, T., Sandhoff, K., 2010. Lysosomal degradation of membrane lipids. FEBS Lett. 584, 1700–1712.
Li, G., Shen, B., He, N., Ma, C., Elingarami, S., Li, Z., 2011. Synthesis and characterization of Fe3O4@ SiO2 core–shell magnetic microspheres for extraction of genomic DNA from human whole blood. J. Nanosci. Nanotechnol. 11, 10295–10301.
Lieckfeldt, R., Villalaín, J., Gómez-Fernández, J.C., Lee, G., 1995. Apparent pKa of the fatty acids within ordered mixtures of model human stratum corneum lipids. Pharm. Res 12, 1614–1617.
Liu, J.-H., Cao, L., LeCroy, G.E., Wang, P., Meziani, M.J., Dong, Y., Liu, Y., Luo, P.G., Sun, Y.-P., 2015. Carbon "quantum" dots for fluorescence labeling of cells. ACS Appl. Mater. Interfaces 7, 19439–19445.
Maeda, Y., Toyoda, T., Mogi, T., Taguchi, T., Tanaami, T., Yoshino, T., Matsunaga, T., Tanaka, T., 2016. DNA recovery from a single bacterial cell using charge-reversible magnetic nanoparticles. Colloids Surf. B: Biointerfaces 139, 117–122.
Mohsen Dehnavi, S., Pazuki, G., Vossoughi, M., 2015. PEGylated silica-enzyme nanoconjugates: a new frontier in large scale separation of α-amylase. Sci. Rep. 5, 18221.
Moradi, S., Najjar, R., Hamishehkar, H., Lotfi, A., 2022. Triple-responsive drug nanocarrier: magnetic core-shell nanoparticles of Fe3O4@ poly (N-isopropylacrylamide)-grafted-chitosan, synthesis and in vitro cytotoxicity evaluation against human lung and breast cancer cells. J. Drug Deliv. Sci. Technol., 103426.
Naahidi, S., Jafari, M., Edalat, F., Raymond, K., Khademhosseini, A., Chen, P., 2013. Biocompatibility of engineered nanoparticles for drug delivery. J. Control. Release 166, 182–194.
Pan, X., Cheng, S., Su, T., Zuo, G., Zhang, C., Wu, L., Jiao, Y., Dong, W., 2019. Poly (2-hydroxypropylene imines) functionalized magnetic polydopamine nanoparticles for high-efficiency DNA isolation. Appl. Surf. Sci. 498, 143888.
Perçin, I., Karakoç, V., Akgöl, S., Aksöz, E., Denizli, A., 2012. Poly (hydroxyethyl methacrylate) based magnetic nanoparticles for plasmid DNA purification from Escherichia coli lysate. Mater. Sci. Eng.: C. 32, 1133–1140.
Pérez, A.G., González-Martínez, E., Águila, C.R.D., González-Martínez, D.A., Ruiz, G.G., Artalejo, A.G., Yee-Madeira, H., 2020. Chitosan-coated magnetic iron oxide nanoparticles for DNA and rhEGF separation. Colloids Surf. A: Physicochem. Eng. Asp. 591, 124500.
Puente-Santiago, A.R., Rodríguez-Padrón, D., 2020. Surface-modified Nanobiomaterials for Electrochemical and Biomedicine Applications. Springer,.
Rahnamaee, S.Y., Ahmadi Seyedkhani, S., Eslami Saed, A., Sadrnezhaad, S.K., Seza, A., 2022. Bioinspired TiO2/chitosan/HA coatings on Ti surfaces: biomedical improvement by intermediate hierarchical films. Biomed. Mater. 17, 035007.
Rendleman, J.A., 1973. Ionization of Carbohydrates in the Presence of Metal Hydroxides and Oxides.
Resch-Genger, U., Grabolle, M., Cavaliere-Jaricot, S., Nitschke, R., Nann, T., 2008. Quantum dots versus organic dyes as fluorescent labels. Nat. Methods 5, 763–775.
Rezaei, A., Ehtesabi, H., 2022. Fabrication of alginate/chitosan nanocomposite sponges using green synthesized carbon dots as potential wound dressing. Materials Today. Chemistry 24, 100910.
Saraji, M., Yousefi, S., Talebi, M., 2017. Plasmid DNA purification by zirconia magnetic nanocomposite. Anal. Biochem. 539, 33–38.
Sosa-Acosta, J.R., Silva, J., Fernández-Izquierdo, L., Díaz-Castañón, S., Ortiz, M., Zuaznabar-Gardona, J.C., Díaz-García, A., 2018. Iron oxide nanoparticles (IONPs) with potential applications in plasmid DNA isolation. Colloids Surf. A: Physicochem. Eng. Asp. 545, 167–178.
Sun, X.-Y., Li, P.-Z., Ai, B., Wang, Y.-B., 2016. Surface modification of MCM-41 and its application in DNA adsorption. Chin. Chem. Lett. 27, 139–144.
Tang, D.-c, DeVit, M., Johnston, S.A., 1992. Genetic immunization is a simple method for eliciting an immune response. Nature 356, 152–154.
Tran, H.N., You, S.-J., Hosseini-Bandegharaei, A., Chao, H.-P., 2017. Mistakes and inconsistencies regarding adsorption of contaminants from aqueous solutions: a critical review. Water Res. 120, 88–116.
Tuerhong, M., Yang, X., Xue-Bo, Y., 2017. Review on carbon dots and their applications. Chin. J. Anal. Chem. 45, 139–150.
Wang, H., Shen, J., Li, Y., Wei, Z., Cao, G., Gai, Z., Hong, K., Banerjee, P., Zhou, S., 2014. Magnetic iron oxide–fluorescent carbon dots integrated nanoparticles for dual-modal imaging, near-infrared light-responsive drug carrier and photothermal therapy. Biomater. Sci. 2, 915–923.
Wang, J., Qiu, J., 2016. A review of carbon dots in biological applications. J. Mater. Sci. 51, 4728–4738.
Wolff, J.A., Malone, R.W., Williams, P., Chong, W., Acsadi, G., Jani, A., Felgner, P.L., 1990. Direct gene transfer into mouse muscle in vivo. Science 247, 1465–1468.
Yıldırım, E., Arıkan, B., Yücel, O., Çakır, O., Kara, N.T., İyim, T.B., Gürdağ, G., Emik, S., 2022. Synthesis and characterization of amino functional poly (acrylamide) coated Fe3O4 nanoparticles and investigation of their potential usage in DNA isolation. Chem. Pap. 1–13.
Zasońska, B., Horák, D., 2022. Magnetic Iron Oxide Particles for Theranostics. Biomedical Nanomaterials. Springer,, pp. 95–115.
Zhang, M., Li, L., Li, B., Tian, N., Yang, M., Zhang, H., You, C., Zhang, J., 2019. Adsorption of DNA by using polydopamine modified magnetic nanoparticles based on solid-phase extraction. Anal. Biochem. 579, 9–17.
Zhang, Y., Zhang, B.-T., Teng, Y., Zhao, J., Kuang, L., Sun, X., 2021. Activation of persulfate by core–shell structured Fe3O4@C/CDs-Ag nanocomposite for the efficient degradation of penicillin. Sep. Purif. Technol. 254, 117617.
Zhu, A., Yuan, L., Liao, T., 2008. Suspension of Fe3O4 nanoparticles stabilized by chitosan and o-carboxymethylchitosan. Int. J. Pharm. 350, 361–368.